

Density Functional Studies of Dicobalt Octacarbonyl-Mediated Azobenzene Formation from 4-Ethynylaniline

Yi-Luen Huang and Fung-E Hong*^[a]

Abstract: Two adiabatic potential-energy surfaces are employed for probing the processes of $[\text{Co}_2(\text{CO})_8]$ -mediated $\text{C}_6\text{H}_5\text{N}=\text{NC}_6\text{H}_5$ formation from $\text{NH}_2\text{C}_6\text{H}_5$. Elementary steps, including oxidative addition of the coordinated amine proton to the cobalt center, reductive elimination of H_2 , CO association, and the coupling process of the diamino fragments, are modeled and examined by using DFT methods at the B3LYP/631LAN level. The formation of $\text{C}_6\text{H}_5\text{N}=\text{NC}_6\text{H}_5$ from $\text{NH}_2\text{C}_6\text{H}_5$ through reductive coupling is a thermo-

dynamically unfavorable process. Three hydride-migration processes, from the proton of N–H to the cobalt center, are established as the most energy-demanding steps. The activation energies (ΔG^\ddagger) are calculated as 49.4, 55.4, and 33.3 kcal mol⁻¹, respectively, for the proposed reaction **route 1**. These large activation energies might be reduced

slightly by purposely adding small protic molecules, such as H_2O , or by changing the active metal from Co to a heavier metal, such as Rh or Ir. An alternative pathway, **route 2**, is also proposed, in which transition states with four-membered rings are formed. By this route, severe strain caused by the formation of three-membered rings during the hydride-migration processes in **route 1** can be avoided. **Route 2** is established as the more energy-feasible reaction pathway.

Keywords: amines • azo compounds • cobalt • density functional calculations • hydride migration

Introduction

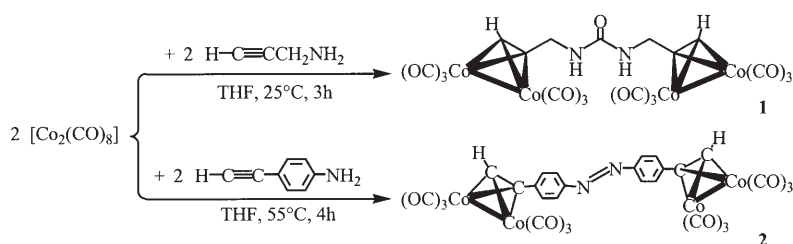
Because the N–H bond is intrinsically strong, its cleavage is a rather energy-demanding process (~ 90 kcal mol⁻¹). Therefore, options of activating the primary or secondary amine have received increasing attention.^[1] Normally, it is through the oxidative addition of the N–H bond to a low-valent transition-metal center that the activation energy can be reduced. Indeed, the participation of a low-valent transition metal in the catalytic cycle is a critical step for many reactions, such as alkene hydroamination,^[2,3] aryl amination,^[4] and imine hydrogenation.^[5] Although the oxidative addition of the N–H bond onto various heavy transition metals has been reported, it is relatively rare for the first-row transition-metal complexes.^[6,7]

In previous studies, we demonstrated an unusual carbonylation reaction of the primary amine propargylamine $\text{HC}\equiv\text{CCH}_2\text{NH}_2$ by utilizing $[\text{Co}_2(\text{CO})_8]$ as a reaction promoter (Scheme 1).^[8] This reaction was carried out at 25 °C for 3 h in THF and gave $[[\{\text{Co}_2(\text{CO})_6(\mu\text{-HC}\equiv\text{C-})\}\text{CH}_2\text{NH}\}_2\text{C}=\text{O}]$ **1** in 40% yield. A proposed mechanism for the formation of **1** was carefully examined by means of DFT.^[9] Furthermore, replacement of the propargylamine by the 4-ethynylaniline $\text{HC}\equiv\text{CC}_6\text{H}_4\text{NH}_2$ resulted in an azobenzene derivative, $[[\{\text{Co}_2(\text{CO})_6(\mu\text{-HC}\equiv\text{C-})\}\text{-C}_6\text{H}_4\text{N}=\}]_2$ **2**, in 18% yield after reaction at 55 °C for 4 h in THF.^[10] As shown, the formation of **2** requires more severe conditions and the yield is lower than that of **1**. Complex **2** can be regarded as an organometallic version of a potential organic liquid-crystal raw material.^[11,12]

To understand this reaction more fully, a comprehensive knowledge of the reaction route, or reaction mechanism, is required. Unfortunately, most of the conventional experimental methods do not always provide conclusive evidence concerning reaction pathways. Computational quantum techniques are regarded as a promising alternative^[13] and have gradually emerged as a useful complementary tool to previously existing experimental means.^[14] Recently, the density functional theory (DFT) method, with greater computational efficiency than the conventional Hartree–Fock ab

[a] Y.-L. Huang, Prof. F.-E. Hong
Department of Chemistry, National Chung Hsing University
Taichung 40227 (Taiwan)
Fax: (+886) 4-2286-2547
E-mail: fehong@dragon.nchu.edu.tw

Supporting information for this article is available on the WWW under <http://www.chemeurj.org/> or from the author: Tables containing coordinates and energies of the optimized stationary points are available.



Scheme 1. The formation of **1** and **2**.

initio method, has been applied extensively to transition-metal complexes and has gained broad acceptance among both theoretical and experimental chemists.^[15]

To our knowledge, a comprehensive computational examination of the catalytic process in the formation of an azobenzene derivative has not yet been reported. Therefore, a thorough study of the formation of $C_6H_5N=NC_6H_5$, mimicking **2**, from the $[Co_2(CO)_8]$ -mediated coupling reaction of $NH_2C_6H_5$ was pursued by using computational quantum techniques. For computing efficiency, the primary amine $NH_2C_6H_5$ was selected to replace the cumbersome 4-ethynylaniline-bridged dicobalt complex $[Co_2(CO)_6(\mu-HC\equiv CC_6H_4NH_2)]$.^[16]

Computational Methods

All calculations were carried out by using Gaussian 03,^[17] in which the tight criterion (10^{-8} hartree) is the default for the self-consistent-field (SCF) convergence. The molecular geometries were fully optimized under C_1 symmetry, in which the Becke3LYP^[18] functional was used. The LANL2DZ including the double- ζ basis sets for the valence and outermost-core orbitals combined with pseudopotential were used for Co,^[19,20] and 6-31G(d) basis sets were used for the other atoms. This combination is denoted 631LAN, which has proven to be successful in describing the cobalt-mediated Pauson–Khand reaction.^[21] All the stationary points found were characterized as minima (number of imaginary frequency $N_{imag}=0$) and transition states ($N_{imag}=1$) by performing harmonic vibrational frequency analysis. For the determination of transition-state geometry, isothermal relaxation current (IRC)^[22] analyses were used to monitor geometry optimization, to ensure that the transition structures are smoothly connected by two proximal minima along the reaction coordinate. The transition structure (TS) calculations of hydride migration assisted by H_2O were performed by using the quadratic synchronous transit (OST2) method. Thermodynamic quantities, the calculated electronic energies, the enthalpies of reaction ΔH_R , and the activation free energies ΔG^* , were obtained and corrected at constant pressure and 298 K. Stability analysis^[23] was performed to determine if the Kohn–Sham (KS) solutions were stable with respect to variations, which break spin and spatial symmetry.

Results and Discussion

The two most probable reaction routes for the formation of $C_6H_5N=NC_6H_5$ through cobalt-mediated coupling of $NH_2C_6H_5$ are proposed: **route 1** is termed a three-membered-ring pathway, and **route 2**, a four-membered-ring pathway. As shown below, these two routes are constructed from successive elementary steps.

Route 1: Three-membered-ring pathway

A reaction mechanism employing a monomeric cobalt moiety as the acting catalytic species was proposed. This was used to accommodate a probable reaction route (**route 1**) for the formation of an azobenzene derivative, $[[[Co_2(CO)_6(\mu-HC\equiv C-)]-C_6H_4N=]_2]$ **2**, through cobalt-mediated coupling of $NH_2C_6H_4C\equiv CH$. As shown in Figure 1, the mechanism is composed of 11 consecutive elementary reactions:

- π -bridging of a 4-ethynylaniline onto a dicobalt fragment accompanied by the release of 2 molar equivalents of carbonyl groups
- generation of a side product $[CoH(CO)_4]$ and the catalyst precursor $[Co(CO)_4(NHX)]$ (X: $[Co_2(CO)_6(\mu-HC\equiv CC_6H_4-)]$), which is ready for further steps
- release of another molar equivalent of CO
- association of an additional NH_2X molecule with the cobalt center
- N–H oxidative addition (or hydride migration) from the newly coordinated NH_2X to the cobalt center
- release of another molar equivalent of carbonyl species
- a second hydride migration from one coordinated NHX to the cobalt center
- reductive elimination of one molar equivalent of H_2
- hydride migration for the third time
- coordination of a carbonyl group to the cobalt center
- dissociation of the azobenzene derivative **2** along with the active species $[CoH(CO)_3]$.

Because the validity of the first four processes, steps a–d, are well accepted both experimentally and theoretically, our computational studies focus on steps e–k.^[24]

Hydride migration from the coordinated amine and the release of CO: Figure 2 depicts the geometry-optimized molecular structures, including transition states, from **1CP** to **3CP**. The outward appearance of **1CP** is a distorted trigonal-bipyramidal (TBP) structure. An approximate octahedron (Oh) is apparent for **2CP** if taking the hydride into consideration. In the process of **1CP**→**1TS**→**2CP**, an N–H bond is broken and at the same time a Co–H bond is formed. The Ha (from N2) transfers to the Co center and forms a new Co–H bond; meanwhile, the bond angle of $\angle N2-Co-Ha$ changes from 57° in **1TS** to 87.3° in **2CP**. The bonding mode of N2–Ha towards Co in **1TS** might be best described as agostic bonding.^[25] The bond length of Co–N2 decreases considerably from 2.399 to 1.944 Å, and then lengthens slightly to 1.996 Å for **1CP**, **1TS**, and **2CP**, respectively. As calculated, the activation free energy for the hydride-migration step (e), **1CP**→**1TS**, is rather high (ca. 49.4 kcal mol⁻¹). It has been shown elsewhere that activation

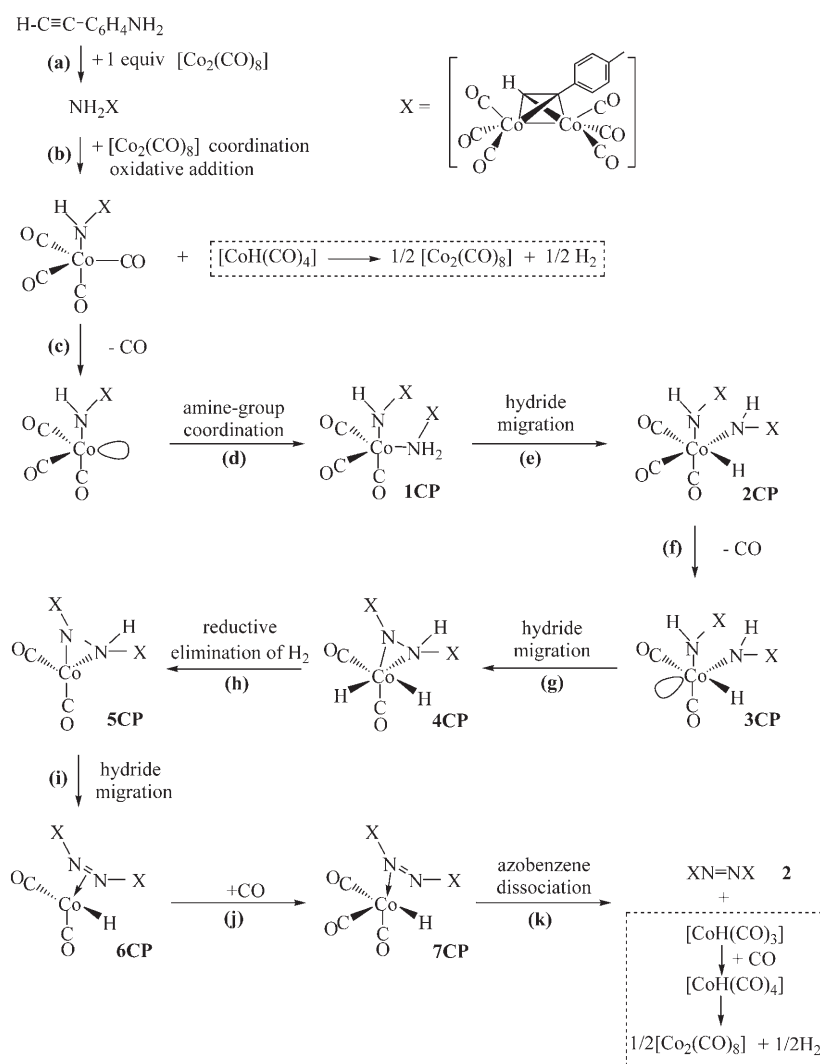


Figure 1. The formation of an azobenzene derivative **2**: **Route 1**.

of the N–H bond is an energy-demanding process mediated by a low-valent metal complex.^[26] As described below for all the elementary steps, these types of hydride-migration processes represent the most crucial steps in the cobalt-mediated formation of azobenzene. For **2CP**→**2TS**→**3CP**, a carbonyl is released from **2CP** and a distorted TBP is restored in **3CP**. The Co–CO bond is elongated from 1.852 Å in **2CP** to 2.651 Å in **2TS**. Finally, the coordinated CO is completely released from **2TS**. Interestingly, this CO-releasing process, **2CP**→**2TS**→**3CP**, does not require a great amount of energy (ca. 24.4 kcal mol⁻¹).

Hydride migration from the amino group and the release of H₂: As depicted in Figure 3, the processes of **3CP**→**3TS**→**4CP** are similar to the previous hydride migration, except that the hydride comes from the amino group rather than the coordinated amine. The hydride-migration step, **3CP**→**3TS**, has the highest activation energy (ca. 55.5 kcal mol⁻¹). The bond length of the ready-to-be-released N1–Hb increases

from 1.015 Å (**3CP**) to 1.797 Å (**3TS**); this is then followed by the complete dissociation of the N1–Hb bond and the formation of a Co–Hb bond (**4CP**). The Co–N1 bond is best regarded as a Co=N double bond in **3TS**. Meantime, the Co–Hb bond length is reduced from 1.522 Å (**3TS**) to 1.486 Å (**4CP**). Furthermore, the N1–N2 bond is formed during the processes of **3CP**→**3TS**→**4CP**. This is indicated by both the changes in bond angles of ∠N1–Co–N2 (from 107.2° in **3CP** to 107.0° in **3TS** to 41.8° in **4CP**) and the short bond length of N1–N2 (1.404 Å) in **4CP**.

In **4CP**, the bonding between the cobalt atom and the dinitrogen moiety, diphenylhydrazide, can be regarded as a combination of a covalent and a dative bond. Reports of crystal structures containing triangular MN₂ moieties for the first-row transition-metal complexes are rare,^[27] although many examples for heavy transition metals are known.^[28] The next step is the release of one molar equivalent of H₂ molecules from **4CP** by reductive elimination. The distance between Ha and Hb is shortened from 1.783 Å in **4CP** to 1.356 Å in **4TS**, and

the Co–Ha and Co–Hb bonds are elongated to 1.498 and 1.506 Å, respectively. Furthermore, the bond angle of ∠Ha–Co–Hb is reduced from 73.7° in **4CP** to 53.7° in **4TS**. Finally, the complete elimination of one H₂ molecule from the cobalt fragment is observed in **5CP**. The release of H₂ can be detected experimentally. A rather unusual square-planar (SP) geometry is perceived for the Co^I center of **5CP**, in which N1, N2, Co, C2, and C3 are almost coplanar. The dihedral angle between planes N1–Co–N2 and C2–Co–C3 is only 7.24°.

Amino hydride migration and CO coordination: Figure 4 represents the geometry-optimized molecular structures from **5CP** to **7CP**. A hydride migration from the diphenylhydrazide group on **5CP** is required to produce the desired azobenzene **2**. Interestingly, the activation free energy for the hydride-migration step, **5CP**→**5TS**, is significantly lower (ca. 33.3 kcal mol⁻¹) than the previous two hydride-migration processes. From **5CP** to **6CP**, the bonding between the

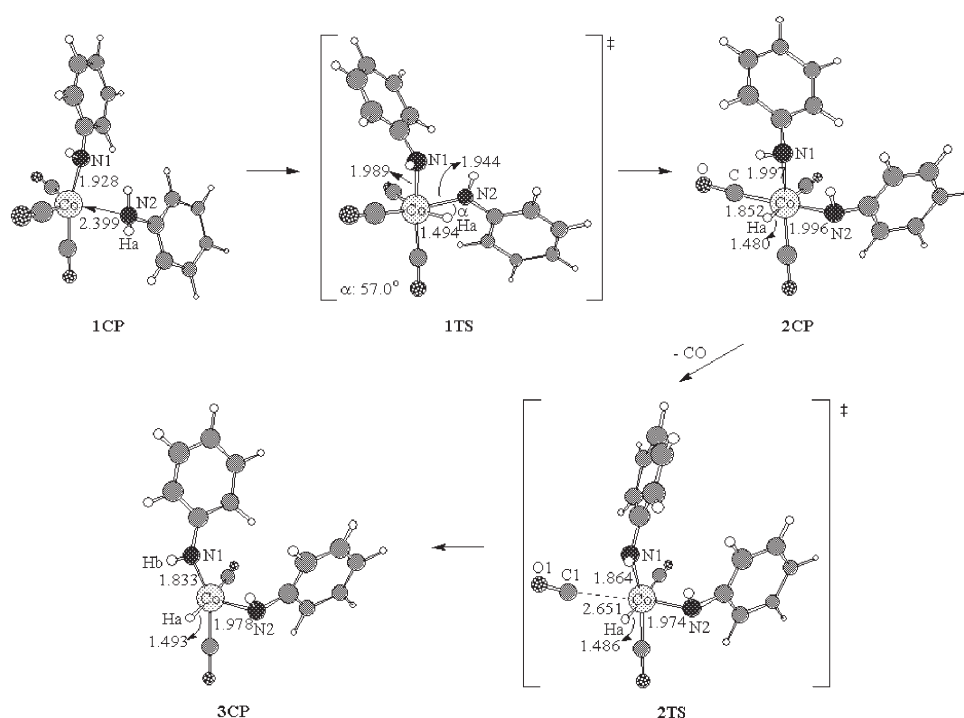


Figure 2. Geometries of stationary points from **1CP** to **3CP** in **route 1**. Distances and angles are in Å and degrees, respectively.

azo moiety and the cobalt fragment changes from a relatively complicated arrangement to a simple L→M dative bond. The bond lengths of Co–N1 and Co–N2 in **5TS** are 2.004

and 2.138 Å, respectively. The corresponding bonds in **6CP** are 2.087 and 2.138 Å. The bond length of N1–N2 is 1.303 Å. In **6CP**, five atoms, N1, Hc, Co, C2, and C3, are almost coplanar. The dihedral angle between planes N1–Co–Hc and C2–Co–C3 is small, 2.64°. **6CP** can be regarded as an unsaturated $[\text{CoH}(\text{CO})_2(\mu\text{-C}_6\text{H}_5\text{N}=\text{NC}_6\text{H}_5)]$. The subsequent steps, **6CP**→**6TS**→**7CP**, represent an external CO coordination to the Co center and the change in bonding mode of the azobenzene ligand $\text{C}_6\text{H}_5\text{N}=\text{NC}_6\text{H}_5$. This leads to the formation of a saturated $[\text{CoH}(\text{CO})_3(\text{L})]$ (L: $\text{C}_6\text{H}_5\text{N}=\text{NC}_6\text{H}_5$) with a TBP shape in **7CP**. Here, the bonding mode of the coordinating ligand $\text{C}_6\text{H}_5\text{N}=\text{NC}_6\text{H}_5$ changes from a π - to a σ -type dative bond. The Co–N1 bond length decreases from 2.087 Å (**6CP**) to 1.957 Å (**6TS**) and then to 2.194 Å (**7CP**). Meanwhile, the bond length of N1–N2 decreases from 1.303 Å in **6CP** to 1.264 Å in **6TS** and then to 1.258 Å in **7CP**. The latter two values

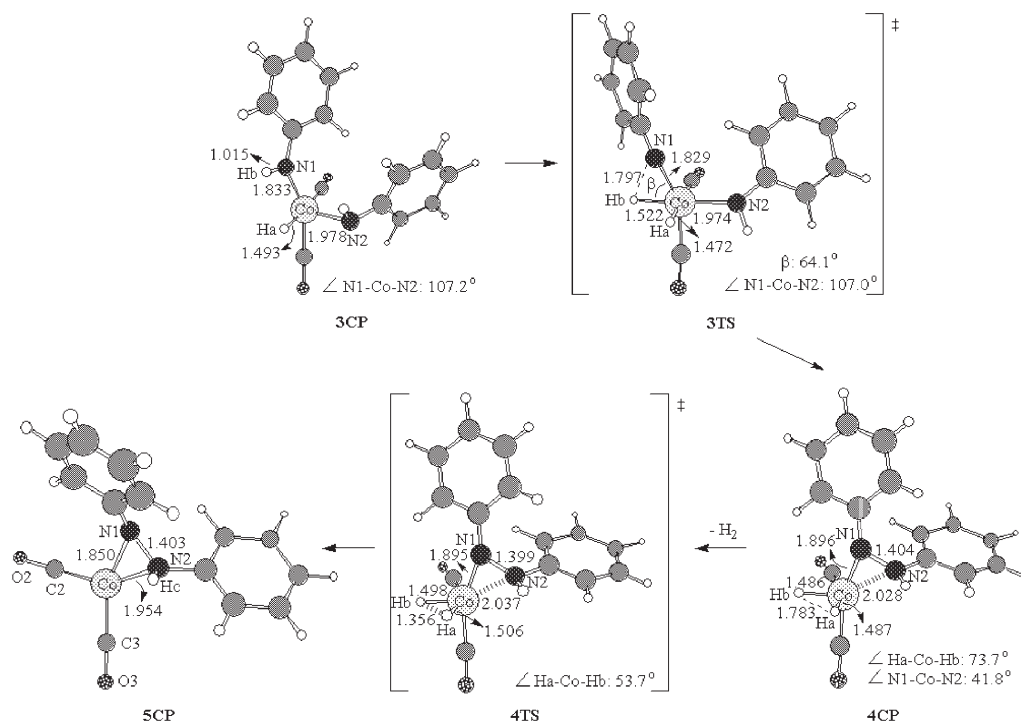


Figure 3. Geometries of stationary points from **3CP** to **5CP** in **route 1**. Distances and angles are in Å and degrees, respectively.

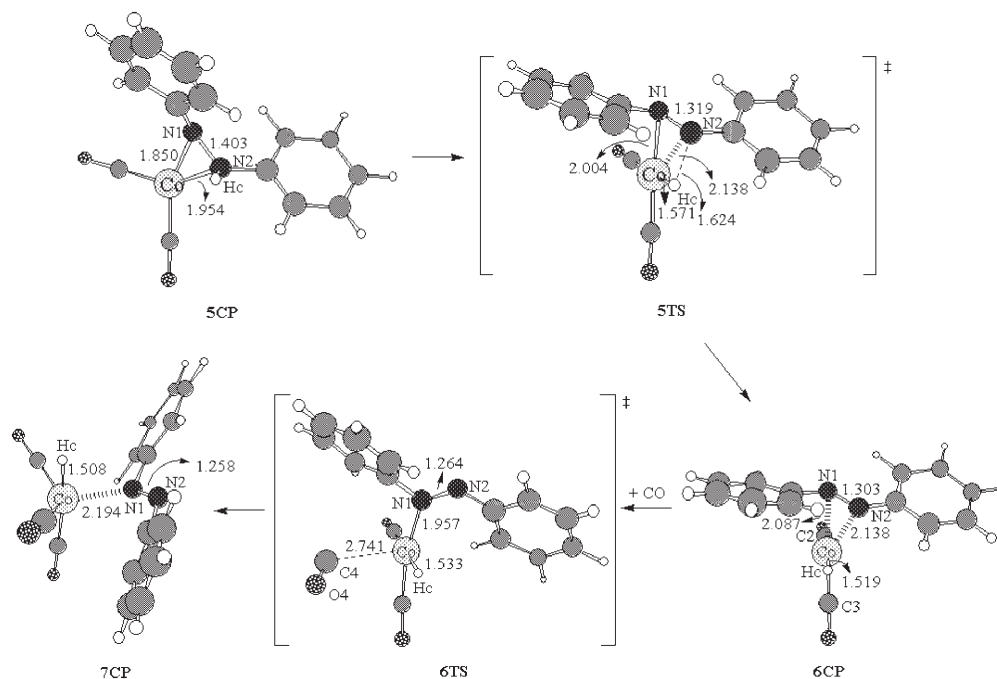


Figure 4. Geometries of stationary points from **5CP** to **7CP** in **route 1**. Distances and angles are in Å and degrees, respectively.

represent the characteristic N=N double bond. A TBP conformation is sustained in **7CP**, with the hydride at one of the axial positions and the azobenzene at one of the equatorial positions.

Potential-energy surface: route 1: The potential-energy surface of the proposed reaction **route 1** is presented in Figure 5. It can be seen that the formation of $C_6H_5N=NC_6H_5$ from $NH_2C_6H_5$ through reductive coupling is a thermodynamically unfavorable process, $\Delta G=41.4 \text{ kcal mol}^{-1}$, and also that the three hydride-migration processes are the most energy-demanding of the steps.

Route 2: Four-membered-ring pathway

As described above, several high-energy-demanding steps in **route 1** are caused by the formation of three-membered rings during the hydride-migration processes. To avoid the severe strain that this induces, an alternative four-membered-ring pathway, **route 2**, is proposed (Figure 6). **Route 2** is constructed from several elementary steps as follows:

- f) coupling of two amino groups by the linking of two nitrogen atoms and breaking of one Co–N bond
- g) hydride migration from amine to cobalt via a four-membered ring containing Co, N1, N2, and Hb atoms, and then formation of another four-membered ring containing Co, N1, N2, and C(C=O) atoms
- h) elimination of one molar equivalent of H_2 from the cobalt center
- i) dissociation of the azobenzene derivative **2**, which is accompanied by the active species $[CoH(CO)_3]$.

Coupling of two amino groups and hydride migration via a four-membered ring: As presented in Figure 7, the initial configuration of **2CPa** is similar to **2CP**, except for the relative positions of the two phenyl groups. Furthermore, **2CP** is slightly more stable than **2CPa** by approximately $3.5 \text{ kcal mol}^{-1}$. During the processes of **2CPa**→**2TSa**→**3CPa**, two amino groups are coupled by the linking of two nitrogen atoms and a diphenylhydrazine moiety is generated. This coupling process proceeds by shortening of the N1–N2 bond (**2TSa**: 1.966 Å and **3CPa**: 1.416 Å) and reduction in the angle of $\angle N1\text{-Co-N2}$ (**2CPa**: 103.5° and **2TSa**: 57.2°). The shape of the molecule changes from Oh for **2CPa** to TBP for **3CPa**. The diphenylhydrazine fragment is situated in one of the equatorial positions and the hydride is located at one of the axial positions.

The **3CPa**→**3TSa**→**4CPa** represents the hydride-migration process. The Hb shifts from the N2 atom to the Co metal by forming a four-membered ring containing Co, N1, N2, and Hb atoms in **3TSa**. Clearly, this conformation assists in reducing the ring strain of the three-membered ring formed in **1TS**. Interestingly, the conformation acquires another four-membered ring containing Co, N1, N2, and C(C=O) atoms in **4CPa**. The length of the N2–Hb bond increases from 1.011 Å in **3CPa** to 1.889 Å in **3TSa**. Meanwhile, the Co–Hb bond length is reduced from 2.952 Å (**3CPa**) to 1.521 Å (**3TSa**). By taking two hydrides into consideration, a distorted Oh is roughly held for **4CPa**. From the view of the three coordinated carbonyl ligands, this is a *fac*-tricarbonylcobalt complex. One of the carbonyl groups interacts with the diphenylhydrazine moiety and forms a C–N bond. This coupling process leads to the formation of a four-membered ring containing Co, N1, N2, and C(CO) atoms.

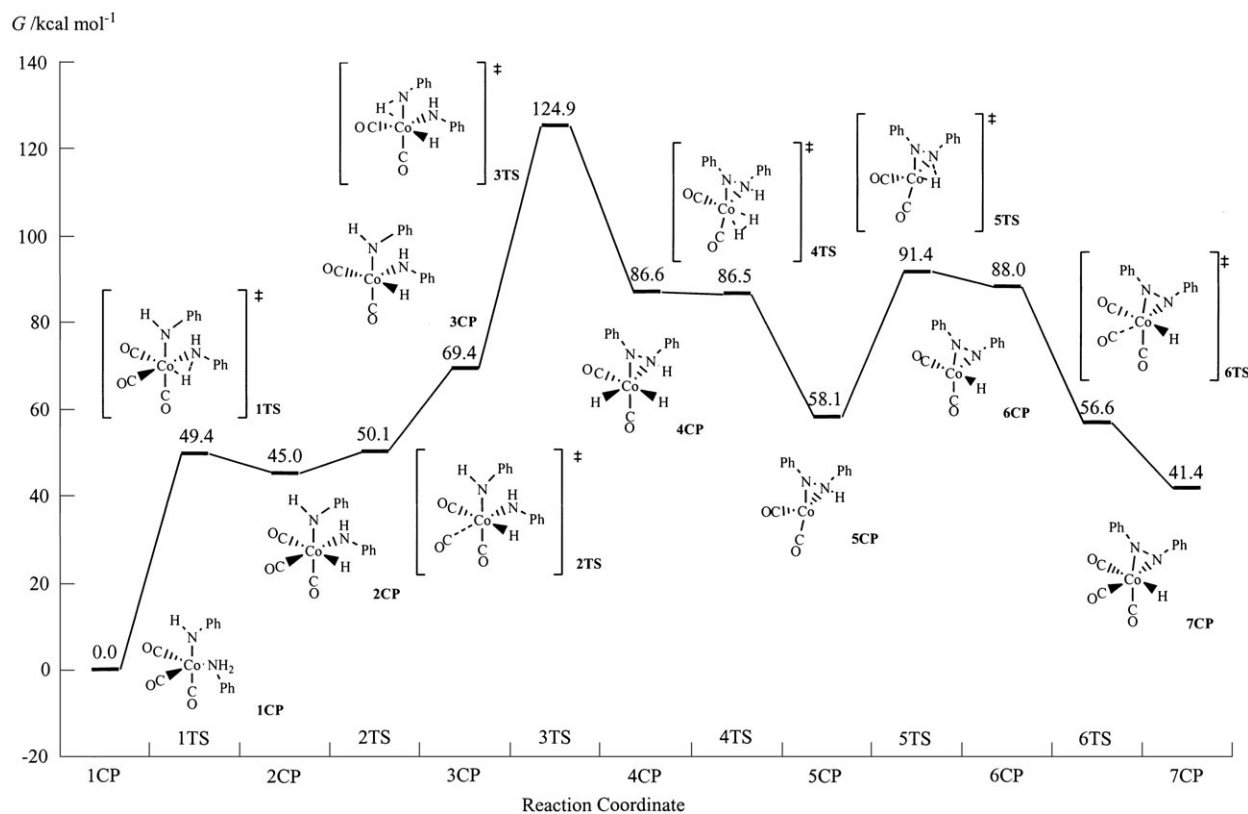


Figure 5. Free energies of transition states involved in **route 1**.

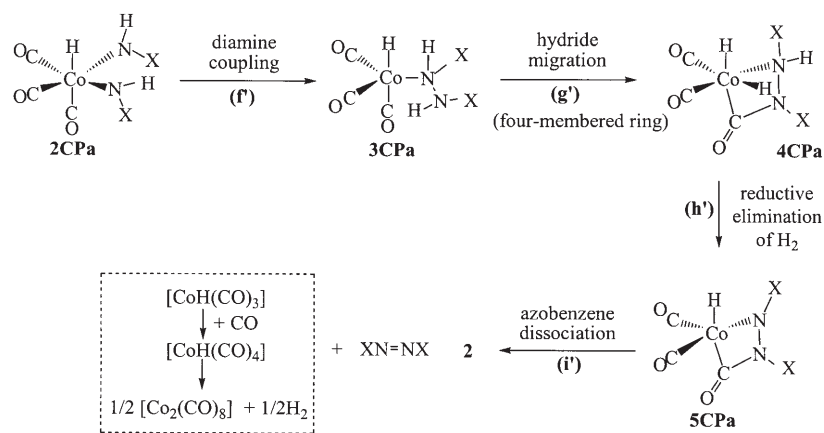


Figure 6. The formation of an azobenzene derivative **2**: **Route 2**.

Hydride migration accompanied by the release of H₂: Similarly, the optimized structures of the process **4CPa** → **4TSa** → **5CPa** are depicted in Figure 8. A hydride migration from the amino group accompanied by the release of one molar equivalent of hydrogen are observed. The Co–N1 bond length is reduced from 2.014 Å (**4CPa**) to 1.972 Å (**4TSa**) and then to 1.804 Å (**5CPa**). The enhanced Co–N1 bond strength assists in stabilizing the electron-unsaturated **5CPa**.

Potential-energy surface: route 2: The potential-energy surface of the proposed **route 2** is presented in Figure 9. The highest activation free energy (ΔG^*) of the corresponding transition state, **3TSa**, is 56.7 kcal mol⁻¹. It is evident that the formation of C₆H₅N=NC₆H₅ from NH₂C₆H₅ through this route is a thermodynamically unfavorable process, and that the hydride-migration processes are the most energy-demanding steps. As a result, **route 2** is established as a more energy-feasible pathway than **route 1**.

Energy comparison for three related reactions: The energies for the formation of three related compounds were calculated and are presented in Table 1. The carbonylation reaction is a thermodynamically favorable process (entry 1, ca. -24.5 kcal mol⁻¹). In contrast, the formation of azobenzene from NH₂C₆H₅ is thermodynamically a rather unfavorable course (entry 2, ca. 61.0 kcal mol⁻¹), which can be made more feasible if a metal-containing species, such as dicobalt-carbonyl, participates in bonding (entry 3, ca. 47.0 kcal

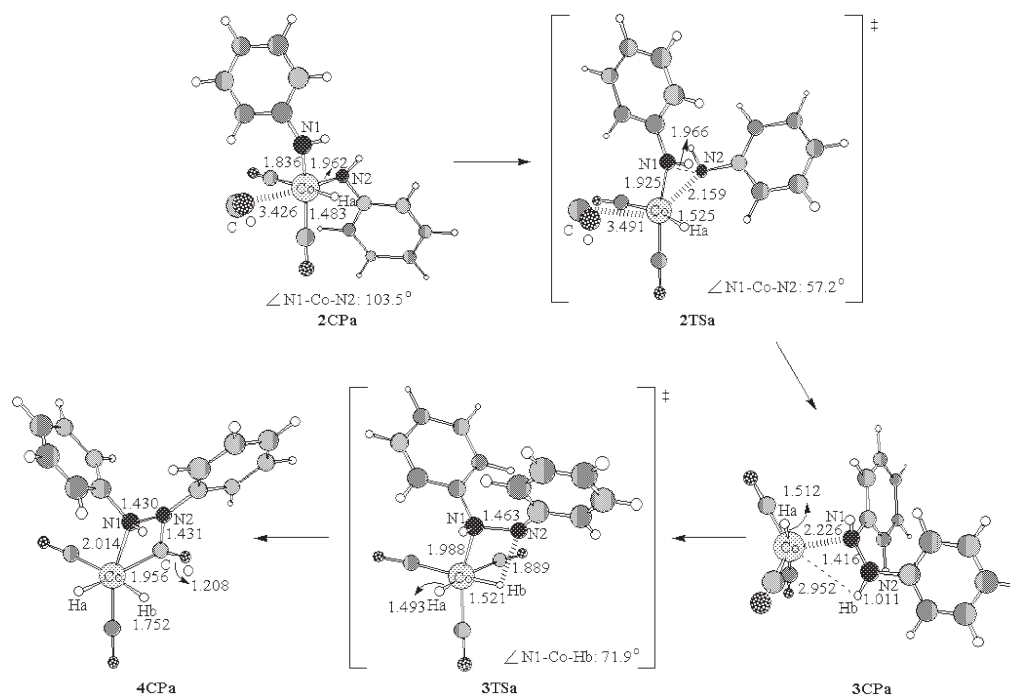


Figure 7. Geometries of stationary points from **2CPa** to **4CPa** in **route 2**. Distances and angles are in Å and degrees, respectively.

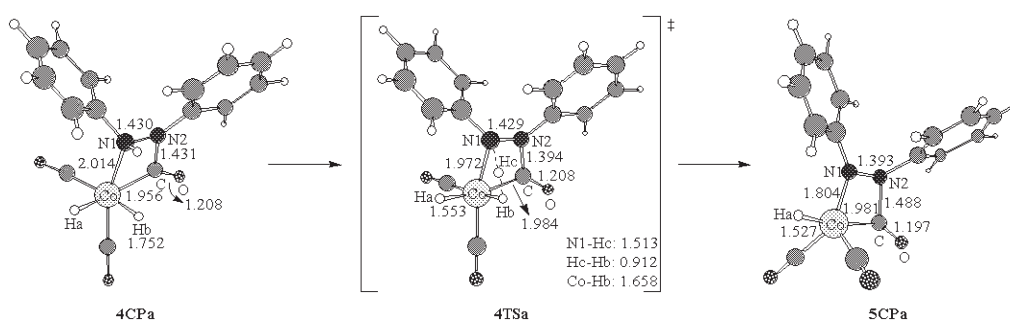


Figure 8. Geometries of stationary points from **4CPa** to **5CPa** in **route 2**. Distances and angles are in Å and degrees, respectively.

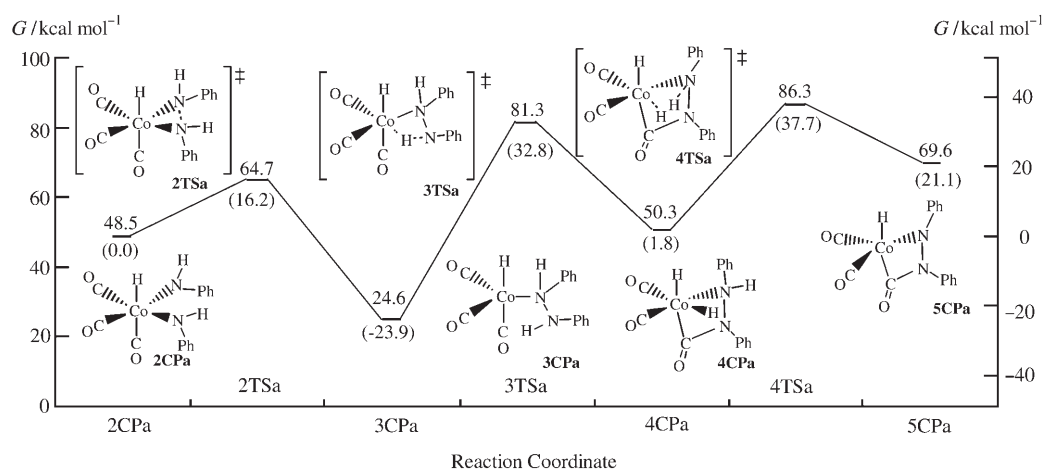
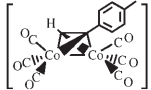


Figure 9. Energy profile for **route 2**. Values of free energies are based on **1CP** (left axis) and **2CPa** (right axis).

Table 1. Reaction enthalpies for the carbonylation, azobenzene formation, and dicobalt-assisted azobenzene formation.

Entry	Reaction	ΔH_R [kcal mol ⁻¹]
1	$2 \text{H}_2\text{N}-\text{CH}_3 + \text{CO} \longrightarrow \text{H}_3\text{C}-\text{N}(\text{H})-\text{C}(=\text{O})-\text{N}(\text{H})-\text{CH}_3 + \text{H}_2$	-24.5
2	$2 \text{H}_2\text{N}-\text{Ph} \longrightarrow \text{Ph}-\text{N}(\text{N})-\text{Ph} + 2 \text{H}_2$	61.0
3	$2 \text{H}_2\text{N}-\text{X} \longrightarrow \text{X}-\text{N}(\text{N})-\text{X} + 2 \text{H}_2$ X = 	47.0

a well-chosen polar and protic solvent might provide an even better environment for lowering the activation free energy.

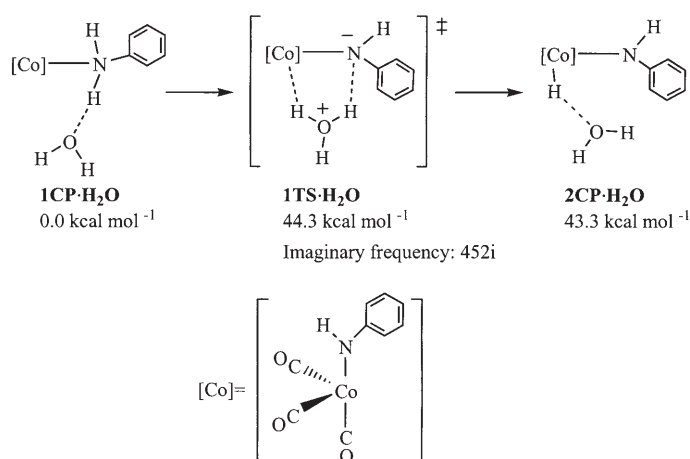
Energy comparison for the hydride-migration process assisted by a Co, Rh, or Ir complex: For comparison, the activation energies and enthalpies for the processes of **1CP**→**1T**→**2CP** with heavy transition metals, such as Rh and Ir, were re-examined

mol⁻¹). Evidently, the dicobaltcarbonyl fragment plays an important role in reducing the reaction enthalpy.

Hydride migration assisted by H₂O: The hydride-migration process was demonstrated to be an energy-demanding process throughout the reaction course. At least two reasons might explain this observation. First, the intrinsically large enthalpy of the N–H bond, making its cleavage difficult; second, the formation of an energetically unfavorable triangular cycle containing Co, N, and H atoms in the transition state. The significant drawback of the latter might be abated by preventing the formation of an energetically unfavorable triangular cycle. A protic molecule, such as H₂O, which is frequently involved in assisting acidification in organic reactions through proton transfer, is employed here to reduce the strain of forming an energetically unfavorable conformation. During actual experimental operations, it is quite possible that a small amount of H₂O indeed dissolves in the polar solvent employed in the reaction.

The hydride-migration process in the presence of H₂O was pursued by using the QST2 method (Scheme 2). The calculated activation free energy for the hydride-migration step with the assistance of H₂O is 44.3 kcal mol⁻¹, which is 5.1 kcal mol⁻¹ lower than for the same step in the absence of H₂O.

The hydride-migration processes of **1CP**·H₂O→**1TS**·H₂O→**2CP**·H₂O that are assisted by H₂O are depicted in Figure 10. As shown, the hydride Ha does not directly migrate from the N2 atom to the Co metal, rather, it transfers firstly from the N2 atom to H₂O. This is then followed by the transfer of He from H₂O to the Co metal. The data show that the Co–N2 bond in **1CP**·H₂O, **1TS**·H₂O, and **2CP**·H₂O is significantly longer than its counterpart in the **1CP**→**1TS**→**2CP** processes: 2.328 Å in **1CP**·H₂O is shortened to 2.042 Å in **1TS**·H₂O and then to 2.006 Å in **2CP**·H₂O. An imaginary frequency in 452i cm⁻¹ is observed for the transition state **1TS**·H₂O. This transition state is a five-membered-ring complex containing Co, N2, Ha, O, and He atoms. As demonstrated, a protic molecule, such as H₂O, indeed provides a lower-energy route, although not significantly lower, for the hydride-migration process. In principle,



Scheme 2. The water-assisted hydride-migration process.

(Scheme 3). As revealed in Table 2, both the activation energy and enthalpy of N–H oxidative addition were reduced (by ca. 5 and 7 kcal mol⁻¹, respectively) by employing a modeled Rh complex. These effects were even greater with a modeled Ir complex (enthalpy reduced by ca. 16 kcal mol⁻¹). This indicates that the amine- or amino-hydride-migration process is more feasible in heavy transition-metal complexes, such as Rh or Ir complexes, than in Co complexes. This has two reasons: first, the larger size of the heavy transition metal atom reduces the strain of the energetically unfavorable triangular cycle containing M, N, and H atoms; second, the availability of more orbitals allows the hybridized orbitals to form acute angles on bonding.

Conclusion

We have explored the reaction pathways of the [Co₂(CO)₈]-mediated N=N coupling reaction from the primary amine NH₂C₆H₅. The proposed reaction routes, **routes 1** and **2**, were examined by utilizing the DFT method at the B3LYP/631LAN level. The N–H oxidative addition processes (hydride migration) were identified as the most energy-demanding steps for both routes. These large energy barriers are responsible for the rigorous reaction conditions required

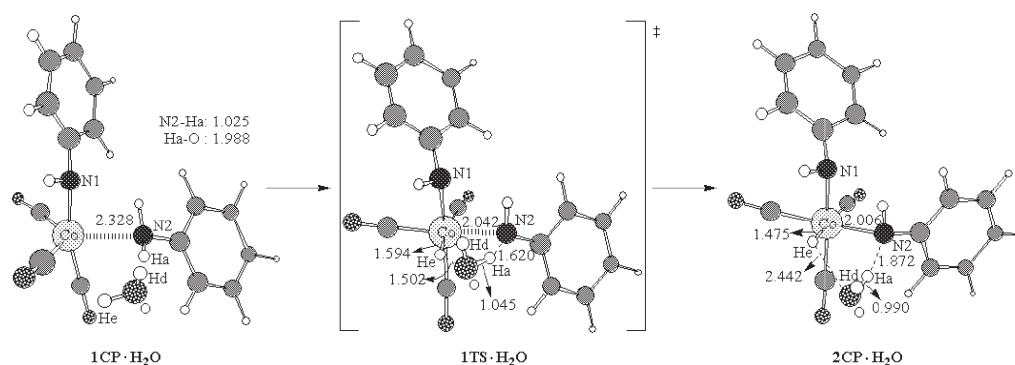
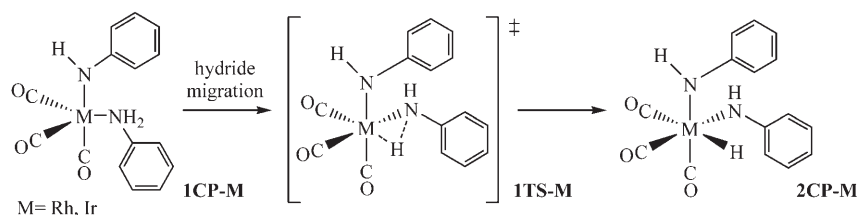


Figure 10. Geometries of stationary points for **1CP·H₂O** to **2CP·H₂O**. Distances and angles are in Å and degrees, respectively.



Scheme 3. The corresponding processes of **1CP**→**1TS**→**2CP** with Rh and Ir metal.

Table 2. Activation energy and enthalpy [kcalmol⁻¹] of N–H oxidative addition to Co, Rh, and Ir model complexes.

Compound	Hartree [a.u.]	[kcal mol ⁻¹] ^[a]
1CP (Co)	−1059.437693	0.00
1TS (Co)	−1059.359021	49.37
2CP (Co)	−1059.365995	45.00
1CP-Rh	−1023.898668	0.00
1TS-Rh	−1023.827682	44.54
2CP-Rh	−1023.837671	38.28
1CP-Ir	−1019.113652	0.00
1TS-Ir	−	−
2CP-Ir	−1019.077646	22.59

[a] All energies are related to **1CP**, which is set as 0.00 kcalmol⁻¹.

in the cobalt-mediated azobenzene-formation reaction. The large activation energies might be reduced by addition of a protic molecule, such as H₂O (reduction ca. 5.1 kcalmol⁻¹), or by changing the active metal to Rh or Ir. To our knowledge, this is the first integrated computational examination of a [Co₂(CO)₈]-mediated dinitrogen coupling reaction from a primary amine.

Acknowledgements

We thank the National Science Council of the R.O.C. (Grant NSC-93–2113-M-005-020) for financial support. The CPU time that was used to complete this project was provided mostly by the National Center for High-Performance Computing (NCHC).

[1] a) M. Kanzelberger, X. Zhang, T. J. Emge, A. S. Goldman, J. Zhao, C. Incarvito, J. F. Hartwig, *J. Am. Chem. Soc.* **2003**, *125*, 13644;

b) M. D. Fryzuk, C. D. Montgomery, *Coord. Chem. Rev.* **1989**, *95*, 1; c) H. E. Bryndza, W. Tam, *Chem. Rev.* **1988**, *88*, 1163.

[2] a) F. Alonso, I. P. Beletskaya, M. Yus, *Chem. Rev.* **2004**, *104*, 3079; b) X. Wang, R. A. Widenhoefer, *Organometallics* **2004**, *23*, 1649; c) C. Cao, Y. Shi, A. L. Odom, *Org. Lett.* **2002**, *4*, 2853; d) Y. Shi, J. T. Ciszewski, A. L. Odom, *Organometallics* **2001**, *20*, 3967; e) T. E. Müller, M. Beller, *Chem.*

Rev. **1998**, *98*, 675; f) J. J. Brunet, *Gazz. Chim. Ital.* **1997**, *127*, 111; g) R. Taube in *Applied Homogeneous Catalysis with Organometallic Compounds* (Eds.: B. Cornils, W. A. Herrmann), VCH, Weinheim, **1996**, p. 507; h) D. M. Roundhill, *Chem. Rev.* **1992**, *92*, 1.

[3] a) M. Beller, H. Trauthwein, M. Eichberger, C. Breindl, J. Herwig, T. E. Müller, O. R. Thiel, *Chem. Eur. J.* **1999**, *5*, 1306; b) M. Beller, H. Trauthwein, M. Eichberger, C. Breindl, T. E. Müller, *Eur. J. Inorg. Chem.* **1999**, 1121; c) M. Beller, H. Trauthwein, M. Eichberger, C. Breindl, T. E. Müller, A. Zapf, *J. Organomet. Chem.* **1998**, *566*, 277; d) M. Beller, M. Eichberger, H. Trauthwein, *Angew. Chem.* **1997**, *109*, 2306; *Angew. Chem. Int. Ed. Engl.* **1997**, *36*, 2225.

[4] a) J. P. Wolfe, S. Wagaw, J.-F. Marcoux, S. L. Buchwald, *Acc. Chem. Res.* **1998**, *31*, 805; b) J. F. Hartwig, *Synlett* **1997**, 329.

[5] a) T. Ohkuma, M. Kitamura, R. Noyori in *Catalytic Asymmetric Synthesis*, 2nd ed. (Ed.: I. Ojima), Wiley-VCH, New York, **2000**; b) A. G. Becalski, W. R. Cullen, M. D. Fryzuk, B. R. James, G.-J. Kang, S. J. Rettig, *Inorg. Chem.* **1991**, *30*, 5002; c) M. D. Fryzuk, W. E. Piers, *Organometallics* **1990**, *9*, 986; d) C. J. Longley, T. J. Goodwin, G. Wilkinson, *Polyhedron* **1986**, *5*, 1625.

[6] G. J. Kubas, *Metal Dihydrogen and π -Bonded Complexes*, Kluwer Academic, New York, **2001**.

[7] a) J. R. Fulton, A. W. Holland, D. J. Fox, R. G. Bergman, *Acc. Chem. Res.* **2002**, *35*, 44, and references therein; b) A. L. Casalnuovo, J. C. Calabrese, D. Milstein, *J. Am. Chem. Soc.* **1988**, *110*, 6738.

[8] F. E. Hong, Y. T. Tsai, Y. C. Chang, B. T. Ko, *Inorg. Chem.* **2001**, *40*, 5487.

[9] F. E. Hong, Y. C. Chang, *Organometallics* **2004**, *23*, 718.

[10] F. E. Hong, C. W. Chen, Y. C. Chang, *J. Chem. Soc. Dalton Trans.* **2002**, *15*, 2951.

[11] a) "Crystal Structures of LC Mesogens": W. Haase, M. A. Athanassopoulou in *Liquid Crystal I* (Ed.: D. M. P. Mingos), Springer, Berlin, Heidelberg, **1999**; b) "Metallomesogens": B. Donnio, D. W. Bruce in *Liquid Crystal II* (Ed.: D. M. P. Mingos), Springer, Berlin, Heidelberg, **1999**.

[12] a) *Solid-State Supramolecular Chemistry: Crystal Engineering in Comprehensive Supramolecular Chemistry* (Eds.: D. D. MacNicol, F. Toda, R. Bishop), Pergamon, Oxford, **1996**, Vol. 6; b) R. Bishop, *Chem. Soc. Rev.* **1996**, *25*, 311; c) Y. Inoue, Y. Sakaino, *Bull. Chem.*

- Soc. Jpn.* **1986**, *59*, 3295; d) Y. Sakaino, T. Takizawa, Y. Inoue, H. Kakisawa, *J. Chem. Soc. Perkin Trans. 2* **1986**, 1623; e) Y. Sakaino, R. Fujii, *J. Chem. Soc. Perkin Trans. 1* **1990**, 2852; f) M. Kaftory, H. Taycher, M. Botoshansky, *J. Chem. Soc. Perkin Trans. 2* **1998**, 407; g) K. Yoshida, Y. Ooyama, S. Tanikawa, S. Watanabe, *Chem. Lett.* **2000**, 714; h) K. Tanaka, M. Asami, J. L. Scott, *New J. Chem.* **2002**, *26*, 378.
- [13] *Computational Modelling of Homogeneous Catalysis* (Eds.: A. Lledós, F. Maseras), Kluwer, Dordrecht, The Netherlands, **2002**.
- [14] a) J. A. Pople, *Angew. Chem.* **1999**, *111*, 2014; *Angew. Chem. Int. Ed.* **1999**, *38*, 1894; b) W. J. Hehre, L. Radom, P. von R. Schleyer, J. A. Pople, *Ab Initio Molecular Orbital Theory*, Wiley, New York, **1986**; c) W. Koch, M. C. Holthausen, *A Chemist's Guide to Density Functional Theory*, Wiley-VCH, Weinheim, **2000**.
- [15] a) T. Ziegler, *Chem. Rev.* **1991**, *91*, 651; b) E. R. Davidson, *Chem. Rev.* **2002**, *102*, 351.
- [16] F. E. Hong, Y. L. Huang, Y. C. Chang, K. M. Chu, Y. T. Tsai, *Appl. Organomet. Chem.* **2003**, *17*, 458.
- [17] Gaussian 03, Revision C.02, M. J. Frisch, G. W. Trucks, H. B. Schlegel, G. E. Scuseria, M. A. Robb, J. R. Cheeseman, J. A. Montgomery, Jr., T. Vreven, K. N. Kudin, J. C. Burant, J. M. Millam, S. S. Iyengar, J. Tomasi, V. Barone, B. Mennucci, M. Cossi, G. Scalmani, N. Rega, G. A. Petersson, H. Nakatsuji, M. Hada, M. Ehara, K. Toyota, R. Fukuda, J. Hasegawa, M. Ishida, T. Nakajima, Y. Honda, O. Kitao, H. Nakai, M. Klene, X. Li, J. E. Knox, H. P. Hratchian, J. B. Cross, V. Bakken, C. Adamo, J. Jaramillo, R. Gomperts, R. E. Stratmann, O. Yazyev, A. J. Austin, R. Cammi, C. Pomelli, J. W. Ochterski, P. Y. Ayala, K. Morokuma, G. A. Voth, P. Salvador, J. J. Dannenberg, V. G. Zakrzewski, S. Dapprich, A. D. Daniels, M. C. Strain, O. Farkas, D. K. Malick, A. D. Rabuck, K. Raghavachari, J. B. Foresman, J. V. Ortiz, Q. Cui, A. G. Baboul, S. Clifford, J. Cioslowski, B. B. Stefanov, G. Liu, A. Liashenko, P. Piskorz, I. Komaromi, R. L. Martin, D. J. Fox, T. Keith, M. A. Al-Laham, C. Y. Peng, A. Nanayakkara, M. Challacombe, P. M. W. Gill, B. Johnson, W. Chen, M. W. Wong, C. Gonzalez, J. A. Pople, Gaussian, Inc., Wallingford, CT, **2004**.
- [18] a) A. D. Becke, *J. Chem. Phys.* **1993**, *98*, 5648; b) C. Lee, W. Yang, R. G. Parr, *Phys. Rev. B* **1988**, *37*, 785.
- [19] T. H. Dunning, Jr., P. J. Hay, *Modern Theoretical Chemistry*, Plenum, New York, **1976**, p. 1.
- [20] P. J. Hay, W. R. Wadt, *J. Chem. Phys.* **1985**, *82*, 299.
- [21] M. Yamanaka, E. Nakamura, *J. Am. Chem. Soc.* **2001**, *123*, 1703.
- [22] a) C. Gonzalez, H. B. Schlegel, *J. Chem. Phys.* **1989**, *90*, 2154; b) C. Gonzalez, H. B. Schlegel, *J. Phys. Chem.* **1990**, *94*, 5523.
- [23] a) R. Seeger, J. A. Pople, *J. Chem. Phys.* **1977**, *66*, 3045; b) R. Bauernschmitt, R. Ahlrichs, *J. Chem. Phys.* **1996**, *104*, 9047.
- [24] a) H. Greenfield, H. W. Sternberg, R. A. Friedel, J. H. Wotiz, R. Markby, I. Wender, *J. Am. Chem. Soc.* **1956**, *78*, 120; b) T. M. Wido, G. H. Young, A. Wojcicki, M. Calligaris, G. Nardin, *Organometallics* **1988**, *7*, 452; c) A. Berenbaum, F. Jäkle, A. J. Lough, I. Manners, *Organometallics* **2001**, *20*, 834; d) A. A. Blanchard, P. Gilmont, *J. Am. Chem. Soc.* **1940**, *62*, 1192; e) W. C. Fernelius, *Inorganic Syntheses*, McGraw-Hill, New York, **1946**, p. 238; f) M. Orchin, *Acc. Chem. Res.* **1981**, *14*, 259; g) M. Torrent, M. Solá, G. Frenking, *Chem. Rev.* **2000**, *100*, 439; h) C. F. Huo, Y. W. Li, G. S. Wu, M. Beller, H. Jiao, *J. Phys. Chem. A* **2002**, *106*, 12161.
- [25] a) M. Brookhart, M. L. H. Green, *J. Organomet. Chem.* **1983**, *250*, 395; b) A. J. Schultz, R. G. Teller, M. A. Bend, J. M. Williams, M. Brookhart, W. Lamanna, M. B. Humphrey, *Science* **1983**, *220*, 197.
- [26] a) G. A. Ardizzoia, S. Brenna, G. LaMonica, A. Maspero, N. Masciocchi, M. Moret, *Inorg. Chem.* **2002**, *41*, 610; b) S. A. Macgregor, *Organometallics* **2001**, *20*, 1860, and references therein.
- [27] L. D. Durfee, J. E. Hill, P. E. Fanwick, I. P. Rothwell, *Organometallics* **1990**, *9*, 75.
- [28] a) W. J. Evans, D. K. Drummond, L. R. Chamberlain, R. J. Doedens, S. G. Bott, H. M. Zhang, J. L. Atwood, *J. Am. Chem. Soc.* **1988**, *110*, 4983; b) P. J. Walsh, F. J. Hollander, R. G. Bergman, *J. Am. Chem. Soc.* **1990**, *112*, 894; c) P. J. Walsh, F. J. Hollander, R. G. Bergman, *J. Organomet. Chem.* **1992**, *428*, 13; d) W. J. Evans, G. K. Kohn, V. S. Leong, J. W. Ziller, *Inorg. Chem.* **1992**, *31*, 3592; e) M. A. Aubart, R. G. Bergman, *Organometallics* **1999**, *18*, 811; f) C. H. Zambrano, P. E. Fanwick, I. P. Rothwell, *Organometallics* **1994**, *13*, 1174.

Received: June 29, 2005
Published online: November 18, 2005